European Review for Medical and Pharmacological Sciences 2020; 24: 5018-5027

MiR-185-3p downregulates advanced glycosylation end product receptor expression and improves renal function in diabetic nephropathy mice

X.-X. XUE[1], H.-Q. LEI[1], L. ZHAO[1], X.-Y. WANG[1], Z. WANG[1], L.-Y. XIE[1], J.-H. JIA[2]

[1]Department of Nephrology, Weinan Central Hospital, Weinan, Shaanxi Province, China
[2]Department of Traditional Chinese Medicine, Ankang Hospital of Traditional Chinese Medicine, Ankang, Shaanxi Province, China

Abstract. – OBJECTIVE: To investigate the effects of the downregulation of AGER by miRNA-185-3p on renal function in diabetic nephropathy (DN) mice.

MATERIALS AND METHODS: Mice were divided into normal, model, NC, miR-185-3p mimic, si-AGER, and miR-185-3p mimic + si-AGER groups. Eight weeks following the establishment of the model, various indicators were assessed.

RESULTS: Compared to control groups, miR-185-3p expression, body weight, superoxide dismutase (SOD) content, catalase (CAT) content, proliferation, S-phase ratios, and proliferating cell nuclear antigen (PCNA) expression were significantly lower in all experimental groups, whilst AGER expression, water intake, food intake, urine volume, urine protein content, serum creatinine (Scr), Blood Urea Nitrogen (BUN), MDA content, G0/G1 status, and rates of apoptosis were significantly higher (all $p<0.05$). Compared to the model group, miR-185-3p mimics, si-AGER, and miR-185-3p mimic + si-AGER groups had a significantly higher SOD content, CAT content, proliferation, S phase ratios, PCNA expression and lower AGER expression, water intake, food intake, urine output, urine protein, Scr, BUN, MDA content, G0/G1 ratios, and apoptosis rates (all $p<0.05$). In addition, the effects of the miR-185-3p mimics + si-AGER were superior to miR-185-3p mimics and si-AGER monotherapy groups (both $p<0.05$).

CONCLUSIONS: MiR-185-3p inhibits AGER, downregulates AGER expression, and improves renal function in DN mice.

Key Words:
MiR-185-3p, AGER, Diabetic nephropathy, Renal function, Advanced glycosylation end products.

Introduction

Diabetic nephropathy (DN) is a complication of diabetes mellitus (DM). Diabetes leads to disturbances in renal function and the occurrence of DN[1]. DN leads to chronic renal failure[2], whose mechanisms remain poorly defined[3]. Understanding the pathogenesis of DN can improve renal function injury in DN patients, with far-reaching significance for DN treatment.

Enhanced levels of advanced glycosylation end products (AGEs) are characteristic of DM. The receptor for these products, the advanced glycosylation end product receptor (AGER) is an AGE-binding protein and a member of the immunoglobulin superfamily. AGER possesses intracellular, extracellular and transmembrane domains. As a signal transduction receptor, AGER binds to AGEs on the cell surface and transduces downstream signals that promote renal damage and deterioration[4-8]. MicroRNAs have been intensively investigated in cancer studies[9-13], but their role in DN development is less well-understood. Bioinformatics predicted a miR-185-3p binding site in AGER, and this miRNA inhibits inflammatory response in intestinal diseases. In addition, miR-185-3p expression is downregulated in hypoxic stress, and its upregulation improves oxidative stress in sarcoma cells. MiR-185-3p is significantly downregulated in DM patients and mouse models and promotes cell proliferation and inhibits apoptosis[14-18].

To date, experimental evidence of the interaction between miR-185-3p and AGER and whether miR-185-3p regulates DN through AGER remains unclear. In this study, we established a DN mouse model and through miR-185-3p silencing or overexpression, we explored its relationship with AGER to understand the effects of miR-185-3p on renal function in DN mice.

Materials and Methods

Experimental Animals

Ninety SPF grade healthy male C57BL/6 mice were selected. The mice had an average weight of 22.18 ± 2.19 g and were aged 6 weeks. Animals were provided by the Animal Center of Guangxi

Corresponding Author: Jinhua Jia, MD; e-mail: jiajinhua48ai@163.com

Medical University (animal license number: SCXK Guijian 2015-0027). Using a random number table method, 10 mice were retained as normal controls. The remainder was used as DN models. All mice were raised according to conventional methods. The study was approved by the Animal Ethics Committee of Weinan Central Hospital. Mice were treated according to the National Principles of Laboratory Animal Care and Management.

Dual-Luciferase Reporter System

Potential miR-185-3p-AGER binding sites were identified through TargetScanHuman (www.targetscan.org). The targeting of AGER by miR-185-3p and AGER was verified using the Dual-Luciferase reporter assay system. Mutations in the predicted binding sites of the reporters were constructed: PGL3-AGER wt and PGL3-AGER mut. *Renilla* plasmids and two reporter plasmids were co-transfected into HEK 293T cells with the miR-185-3p and NC plasmids. Luciferase assays were performed 24 h post-transfection. Dual-Luciferase reporter assay kits were purchased from Promega (Madison, WI, USA). Following firefly Luciferase assessments, *Renilla* Luciferase was added, and Luciferase activity measured. Relative Luciferase activity = firefly Luciferase / *Renilla* Luciferase.

Construction of Mice DN Models

The DN model was established by injecting streptozotocin (STZ) intraperitoneally at 50 mg/kg/d for 5 weeks after 1 week of adaptive feeding[19]. One week after the fifth STZ injection, the blood sugar levels were examined. Blood sugar levels ≥ 300 mg/dL were used as markers of successful modeling. Sixty successfully modeled mice were randomly selected for subsequent grouping.

Experimental Grouping and Processing

Mice were divided into the following 6 groups each containing 10 mice: (1) Normal group (normal control mice); (2) Model group (DN model mice); (3) NC group (DN model mice with 20 mg/kg tail vein injections of a negative control vector); (4) miR-185-3p mimics (DN model mice with a 20 mg/kg tail vein injection of miR-185-3p overexpression vector); (5) si-AGER group (DN model mice with a 20 mg/kg tail vein injection of AGER silencing vector); (6) miR-185-3p mimic + si-AGER group (DN model mice with combined treatment of 20 mg/kg tail vein injection of miR-185-3p overexpression plasmid and 20 mg/kg tail vein injection of AGER silencing vector). All vectors were purchased from Thermo Fisher Scientific (Waltham, MA, USA) and injected into the tail veins after modeling (20 nM, 100 μL). Mice in the microRNA-185-3p mimic + si-AGER group were injected with 100 μL of 20 nM microRNA-185-3p mimic vector, followed by 100 μL of 20 nM si-AGER vector. The vectors were injected once a day for a week. After 1 week of injections, renal function and its related indices were investigated. Blood was collected and mice were sacrificed. Kidney tissues were isolated for subsequent experiments.

Detection of General Conditions in Mice

Water intake, body weight, food intake, urine volume, and urinary protein content of mice in each group were measured after 1 week. Mice in each group were placed in metabolic cages (ZS Dichuang Science and Technology Development Co., Ltd., Beijing, China). Water intake, food intake, and urine volume were measuredby measuring cylinder. Serum creatinine (Scr) and blood urea nitrogen (BUN) were detected by enzyme-linked immunosorbent assay (ELISA). The urinary protein levels were measured with commercial kits (SNM297, Biolab, Beijing, China). Urine protein concentrations were deter mined using the full automatic biochemical analyzer. Scr and BUN were determined according to commercial kits (YS01266B, Yaji Biotechnology Co., Ltd., Shanghai, China).

QRT-PCR

Total RNA was extracted using TRIzol (Invitrogen, Calsbad, CA, USA). Total RNA and RNA purity were determined on a Nanodrop 2000 micro-ultraviolet spectrophotometer (1011U, nanodrop, Wilmington, Delaware, USA) by detecting the ratio of A_{260}/A_{230} and A_{260}/A_{280}, respectively. According to the instructions of TaqMan MicroRNA Assays Reverse Transcription Primer system (4427975; Applied Biosystems, Waltham, MA, USA), the transcription was performed to generate cDNA. cDNA was diluted to 50 ng/μL. PCR reactions were performed in a 25 μL reaction volume. The conditions for reverse transcription were 37°C for 30 min, followed by 85°C for 5 s. Primers for miR-185-3p, GAPDH, U6, and AGER were synthesized by Beijing Qingke Biotechnology Co., Ltd. (Beijing, China) (Table I). Quantitative Real Time-PCR (qRT-PCR) was performed (7500, ABI, Waltham, MA, USA). The reaction conditions were as follows: pre-denaturation at 95°C for 10 min, denaturation at 95°C for 10 s, annealing at 60°C for 20 s, and elongation at 72°C

Table I. Primer sequences.

Gene	Primer sequence (5Đ-3Đ)
miR-185-3p	F: GAGGCTGGAGCTCTCAGGCCACCTGCCCAGGGCGACTCCC R: GGGAGTCGCCCTGGGCAGGTGGCCTGAGAGCTCCAGCCTC
AGER	F: CTTGCTCTATGGGGAGCTGTA R: CATCGACAATTCCAGTGGCTG
U6	F: TGTTCCACACTACGCAGTCC R: TTTGTCGTTCCCGTCTCCTG
GAPDH	F: AGGTCGGTGTGAACGGATTTG R: GGGGTCGTTGATGGCAACA

AGER: advanced glycosylation end product receptor.

for 2 min, for 35 cycles. PCR reactions consisted of qRT-PCR forward primer (10 μM) 0.8 μL, qRT-PCR reverse primer (10 μM) 0.8 μL, ROX reference dye II 0.4 μL, SYBR Premix Ex Taq™ II 10 μL, cDNA template 2.0 μL, and sterile purified water 6.0 μL (total volume = 20 μL). The relative expression of microRNA-185-3p was determined using U6 as an internal reference. The relative expression of AGER was determined using GAPDH. The $2^{-\Delta\Delta Ct}$ was used to measure relative gene expression. The formula was as follows: $\Delta\Delta CT = \Delta Ct_{\text{experimental group}} - \Delta Ct_{\text{GAPDH}}$, in which $\Delta Ct = Ct_{\text{target gene}} - Ct_{\text{internal reference}}$. Ct represented the number of amplification cycles.

Western Blotting

Western blotting was used to detect AGER, cleaved caspase-3, p27, caspase-3, and proliferating cell nuclear antigen (PCNA) expression in the kidneys. Renal homogenates were prepared, and the total proteins were extracted from kidney tissue using RIPA buffer (BB-3209; Bebe Biological Co., Ltd., Shanghai, China). The proteins were resolved by sodium dodecyl sulphate-polyacrylamide gel electrophoresis (SDS-PAGE) and transferred to polyvinylidene difluoride (PVDF) membranes. The membranes were probed with anti-rabbit polyclonal antibodies to AGER (1:2,000, ab3611, Abcam, Cambridge, MA, USA), caspase-3 (1:500, ab13847, Abcam, Cambridge, MA, USA), p27 (1:3,000, ab137736, Abcam, Cambridge, MA, USA), Cleaved caspase-3 (1:500, ab49822, Abcam, Cambridge, MA, USA), and GAPDH (1:3,000, ab37168, Abcam, Cambridge, MA, USA) at 4°C in a shaker overnight. Membranes were washed and labeled with Horseradish Peroxidase (HRP)-conjugated goat anti-rabbit IgG (1:10,000, ab6721, Abcam, Cambridge, MA, USA) at 37°C for 2 hours. Membranes were washed 3 times with phosphate-buffered saline (PBS) at room temperature for 5 min and bands were imaged using the enhanced chemiluminescence (ECL) system. The relative protein expression was calculated using the following formula = gray value of protein band / gray value of GAPDH band of the same sample.

Immunofluorescence

Kidney tissues were fixed with 10% neutral buffered formalin and embedded in paraffin. PCNA was fluorescently labeled and the proliferation of renal cells was determined by PCNA expression. Sections were probed with rabbit monoclonal antibodies PCNA (1:200, ab92552, Abcam, Cambridge, MA, USA) for 1 hour at room temperature. Slides were washed with three times in 1×PBS for 5 min. Secondary IgG (1:1,000, ab6708, Abcam, Cambridge, MA, USA) was blocked for 30 minutes and nuclei were stained with DAPI (Invitrogen Molecular Probes, Carlsbad, CA, USA). After 10 min, the slides were washed three times and imaged under a fluorescent microscope (XSP-BM22AY, Shanghai Optical Instrument Factory, Shanghai, China).

Flow Cytometry

Kidney tissues were sectioned with ophthalmic curved scissors and samples were placed onto 60 μm diameter nylon beakers and washed with PBS. The single cells were collected, fixed in 95% ethanol, and washed in PBS. The cells were centrifuged at 1,500 rpm for 5 min and the supernatants were discarded.

For cell cycle determination, the samples were protected from light and 100 μL RnaseA was added in a 37°C water bath. The cells were incubated for 30 min and stained with 400 μL of Propidium Iodide (PI; Sigma-Aldrich, St. Louis, MO, USA). Cell cycle status was assessed by flow cytometry.

For apoptosis assessments, the cells were stained with Annexin-V-fluorescein isothiocya-

nate (FITC) Apoptosis Detection Kits (Sigma-Aldrich, St. Louis, MO, USA) for 15 min at room temperature. The number of apoptotic cells were assessed by flow cytometry.

Statistical Analysis

Data were analyzed and processed using SPSS 21.0 (SPSS Inc., Chicago, IL, USA) software. All measurement data were expressed as the mean ± SD. A One-way ANOVA combined with Bonferroni two-way comparison tests were used for inter-group comparisons. $p<0.05$ was considered statistically significant.

Results

Dual-Luciferase Reporter Assays

We assessed the binding sites between miR-185-3p and AGER through TargetScanHuman (Figure 1a). Targeting of miR-185-3p to AGER was validated through Dual-Luciferase reporter assays (Figure 1b). No significant differences in AGER mut values between NC and miR-185-3p groups were observed ($p>0.05$), but AGER wt values in the miR-185-3p group were significantly lower than the NC group ($p< 0.05$), suggesting that miR-185-3p targets and regulates AGER.

Expression of MiR-185-3p and AGER in Kidney Tissue

Upon comparison to the normal group, miR-185-3p expression significantly decreased, whilst AGER expression significantly increased in all other groups (all $p<0.05$). Compared to the model group, the expression of miRNA-185-3p in the mice of the miR-185-3p mimic and miR-185-3p mimic + si-AGER groups significantly increased, whilst the expression of AGER mRNA significantly decreased (all $p<0.05$). No significant differences in the expression of miRNA-185-3p between the model and si-AGER groups were observed ($p>0.05$), but the expression of AGER mRNA significantly decreased in the si-AGER group ($p<0.05$). Compared to the miR-185-3p mimic and si-AGER groups, the expression of miR-185-3p significantly increased, whilst the expression of AGER significantly decreased in the miR-185-3p mimic + si-AGER group (all $p<0.05$, Figure 1c).

Assessment of AGER Expression

The expression of AGER was significantly higher in all groups *vs.* the normal group (all $p<0.05$). Compared to the model group, AGER expression in the miR-185-3p mimic group, the si-AGER group, and the miR-185-3p mimic + si-AGER group significantly decreased (all $p<0.05$). Compared to the miR-185-3p mimic and si-AGER groups, AGER expression in the miR-185-3p mimic + si-AGER group significantly decreased (both $p<0.05$, Figure 1d-e).

Relevant Indicators of Renal Function in Mice of Each Group

Compared to the normal group, the body weight of other groups significantly declined. However, water intake, food intake, urine volume, urine protein content, Scr, and BUN content all significantly increased (all $p<0.05$). Compared to the model group, no significant differences in body weights of the miR-185-3p mimic, si-AGER, and miR-185-3p mimic + si-AGER groups were observed (all $p>0.05$), whilst water intake, food intake, urine volume, urinary protein content, Scr, and BUN content in the groups declined (all $p<0.05$). Compared to miR-185-3p mimic and si-AGER groups, no significant difference in the body weights of mice in the mi-185-3p mimic + si-AGER group were observed (both $p>0.05$), whilst water intake, food intake, urine volume, urinary protein content, Scr, and BUN content significantly decreased (all $p <0.05$, Figure 2).

Detection of MDA, SOD and CAT and Assessment of Kidney Cell Proliferation

Compared to the normal group, the MDA content significantly increased, whilst SOD and CAT decreased in all other groups (all $p<0.05$). Compared to the model group, MDA content significantly decreased in the miR-185-3p mimic group, the si-AGER group, and the miR-185-3p mimic + si-AGER group, whilst SOD and CAT contents significantly increased in all groups (all $p<0.05$). Compared to the miR-185-3p mimics and the si-AGER group, MDA levels significantly decreased, whilst the content of SOD and CAT significantly increased in the miR-185-3p mimic + si-AGER group (all $p<0.05$, Figure 3a).

Compared to the normal group, the proliferation rates of the kidney cells significantly decreased (all $p<0.05$). Compared to the model group, the proliferation of renal cells significantly increased in the miR-185-3p mimic group, the si-AGER group, and the microRNA-185-3p mimic + si-AGER group (all $p<0.05$). Compared to the miR-185-3p mimic and si-AGER groups, the proliferation rates of renal cells significantly increased in the miR-185-3p mimic + si-AGER group ($p<0.05$, Figure 3b-c).

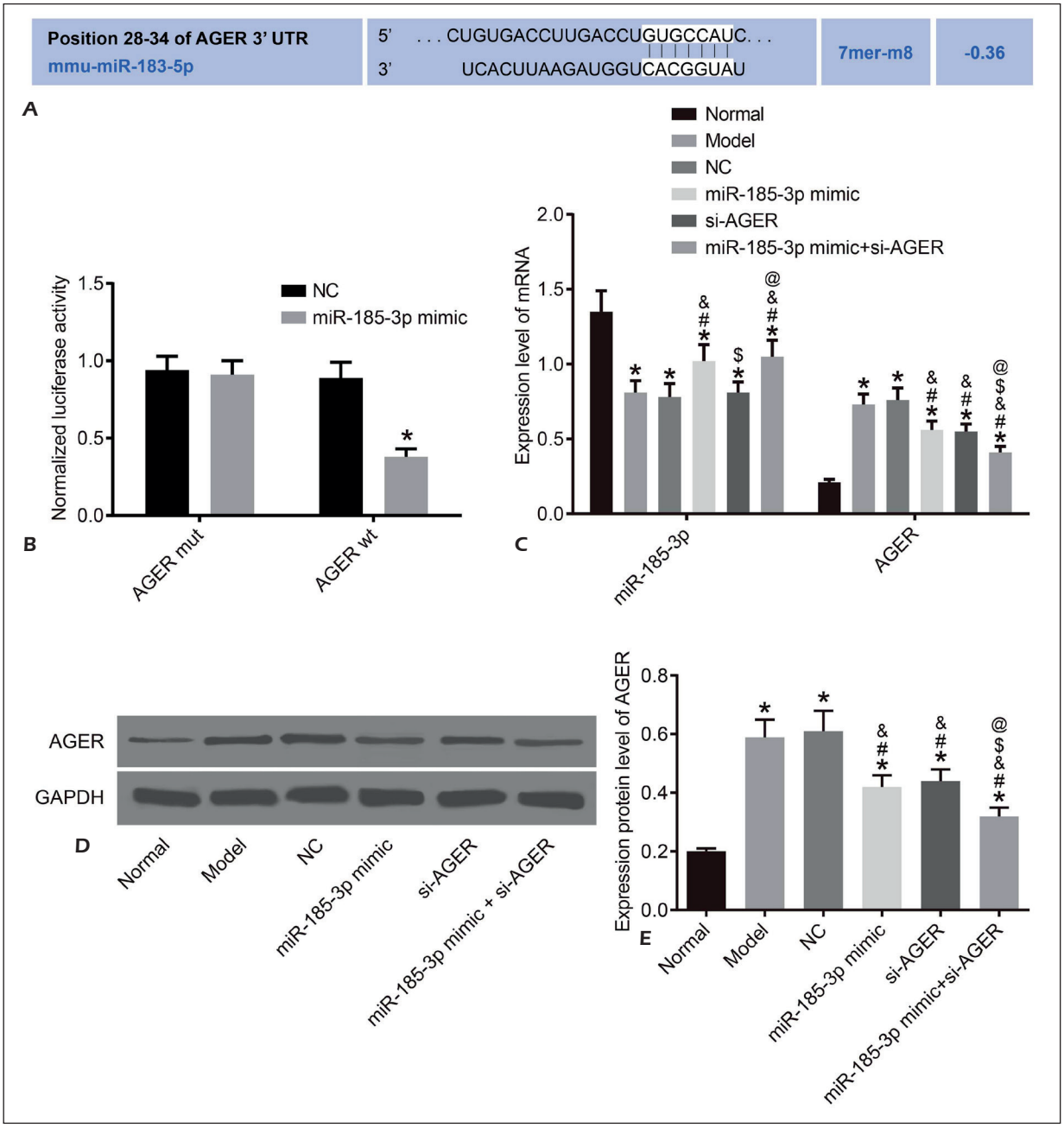

Figure 1. Dual-Luciferase reporter assays and mRNA expression of miR-185-3p, AGER and protein expression of AGER. **A**, Bioinformatics website predicted and analyzed the binding sites between miR-185-3p and AGER. **B**, Dual-Luciferase reporter assay verified the targeting relationship between miR-185-3p and AGER. **C**, Detection of the expression of miR-185-3p and AGER. **D**, Detection of AGER protein expression. **E**, Protein expression of AGER in the kidney of rats in each group. Compared with Normal group, $^{*}p<0.05$. Compared with Model group, $^{\#}p<0.05$. Compared with NC group, $^{\&}p<0.05$. Compared with miR-185-3p mimic group, $^{\$}p<0.05$. Compared with the si-AGER group, $^{@}p<0.05$. AGER: advanced glycosylation end product receptor.

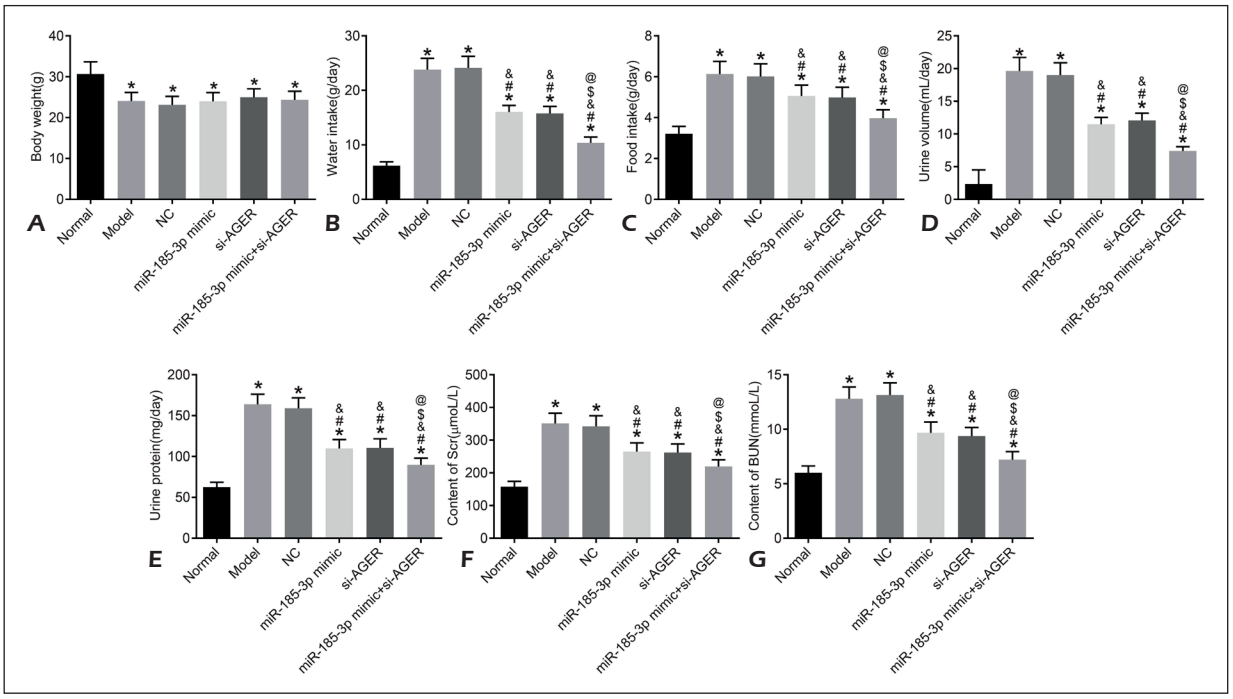

Figure 2. Relevant indicators of renal function in mice of each group. **A**, Comparison of weight in each group. **B**, Comparison of water intake in each group. **C**, Comparison of the intake of mice in each group. **D**, Comparison of urine volume in each group. E, Comparison of urinary protein content in each group. **F**, Comparison of Scr content in each group. **G**, Comparison of BUN content in each group. Compared with Normal group, $^{*}p<0.05$. Compared with Model group, $^{\#}p<0.05$. Compared with NC group, $^{\&}p<0.05$. Compared with miR-185-3p mimic group, $^{\$}p<0.05$. Compared with si-AGER group, $^{@}p<0.05$. AGER: advanced glycosylation end product receptor, Scr: serum creatinine, BUN: blood urea nitrogen.

Assessment of renal Cell Cycle Status, Apoptosis Distribution and Protein Expression in Kidney Tissues

Compared to the normal group, the proportion of cells in the G0/G1 phase significantly increased, whilst the proportion of cells in the S-phase significantly decreased in all other groups (all $p<0.05$). Compared to the model group, the proportion of cells in the G0/G1 phase significantly decreased in the miR-185-3p mimic group, si-AGER group, and miR-185-3p mimic + si-AGER groups, whilst the proportion of cells in the S phase significantly increased in these groups (all $p<0.05$). Compared to the miR-185-3p mimic and si-AGER groups, the proportion of cells in the G0/G1 phase significantly decreased, whilst the proportion of cells in the S-phase significantly increased in the miR-185-3p mimic + si-AGER groups (all $p<0.05$ Figure 4a-b).

In comparison to the normal group, the rates of kidney cell apoptosis significantly increased in all other groups (all $p<0.05$). Compared to the model group, the rates of apoptosis significantly decreased in the miR-185-3p mimic group, si-AGER group, and the miR-185-3p mimic + si-AGER groups (all $p<0.05$). Compared to the miR-185-3pmimic and si-AGER groups, the rates of apoptosis significantly decreased in the miR-185-3p mimic + si-AGER group (all $p<0.05$, Figure 4c-d).

Compared to the normal group, PCNA expression significantly decreased, whilst the expression of caspase-3, p27, and cleaved caspase-3 increased in all other groups (all $p<0.05$). Compared with the model group, PCNA expression significantly increased, whilst the expression of caspase-3, p27 and cleaved caspase-3 significantly decreased in the miR-185-3p mimic group, the si-AGER group, and the miR-185-3p mimic + si-AGER group (all $p<0.05$). Compared to the miR-185-3pmimic and si-AGER groups, PCNA expression significantly increased, whilst the expression of caspase-3, p27, and cleaved caspase-3 significantly decreased in the miR-185-3pmimic + si-AGER groups (all $p<0.05$, Figure 4e-f).

Discussion

DN, as a major complication of DM, causes renal function damage. Long-term DN can lead to renal failure, which seriously endangers the life of patients. Studies on the pathogenesis of DN

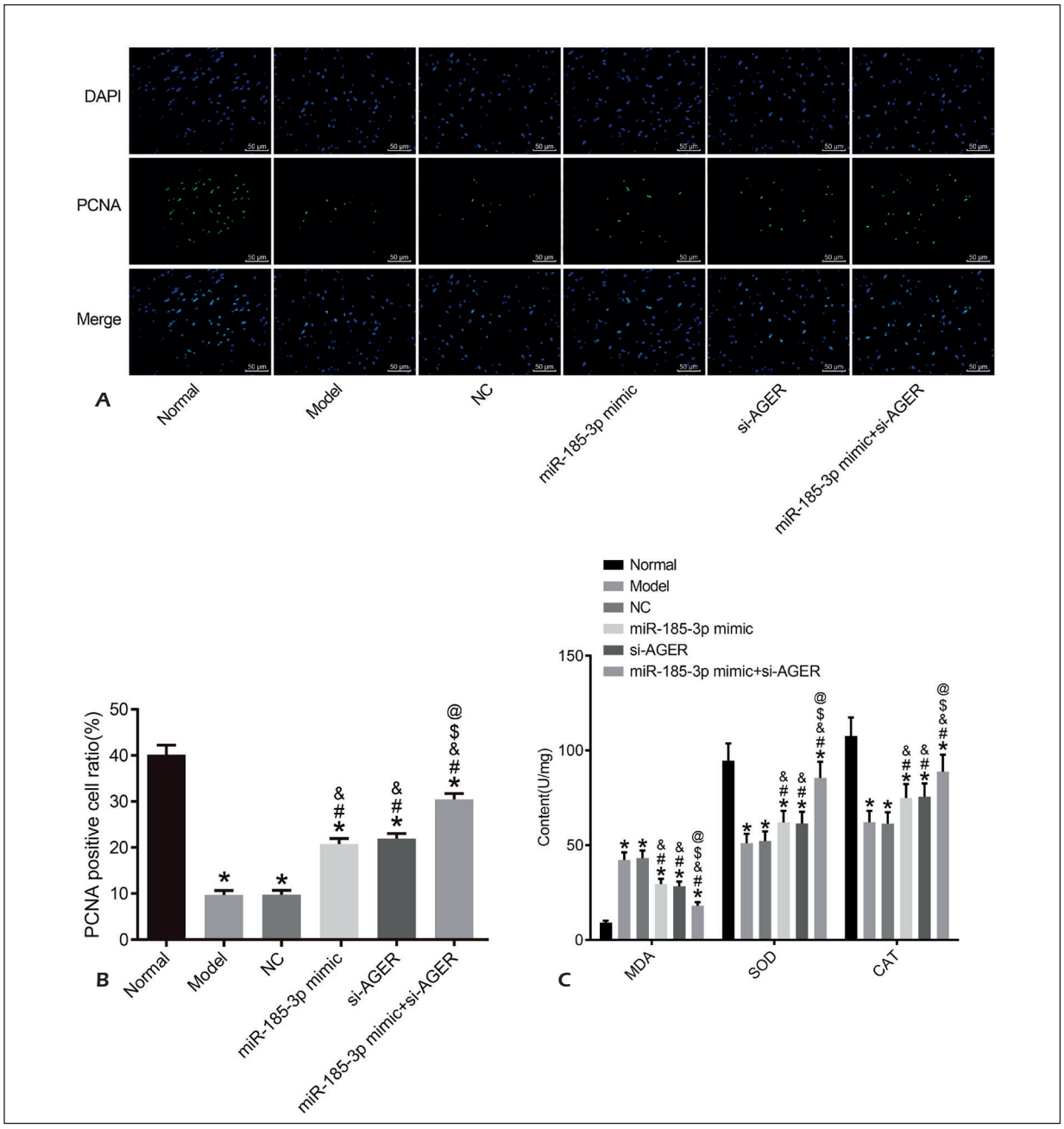

Figure 3. The detection of MDA, SOD, CAT and the assessment of kidney cell proliferation. **A**, Immunofluorescence (200x). **B**, Statistical results of PCNA positive cells proportion. **C**, Detection of MDA, SOD and CAT. Compared with Normal group, $^{*}p<0.05$. Compared with Model group, $^{\#}p<0.05$. Compared with NC group, $^{\&}p<0.05$. Compared with miR-185-3p mimic group, $^{\$}p<0.05$. Compared with si-AGER group, $^{@}p<0.05$. AGER: advanced glycosylation end product receptor, PCNA: proliferating cell nuclear antigen.

are of great significance to effective control and treatment strategies[20-23]. In this study, DN mouse models were used to explore the mechanisms of DN pathogenesis.

MiR-185-3p can inhibit inflammatory responses and oxidative stress induced injury[24-27]. In this study, DN model mice were injected with miR-185-3p mimics, si-AGER, and miR-185-3p mimics + si-AGER vectors. Compared to the normal group, the expression of miR-185-3p in the mouse kidneys significantly decreased. Mice in the miR-185-3p mimic group showed no weight loss, but renal function indices, including water intake, food intake, urine volume, urinary protein con-

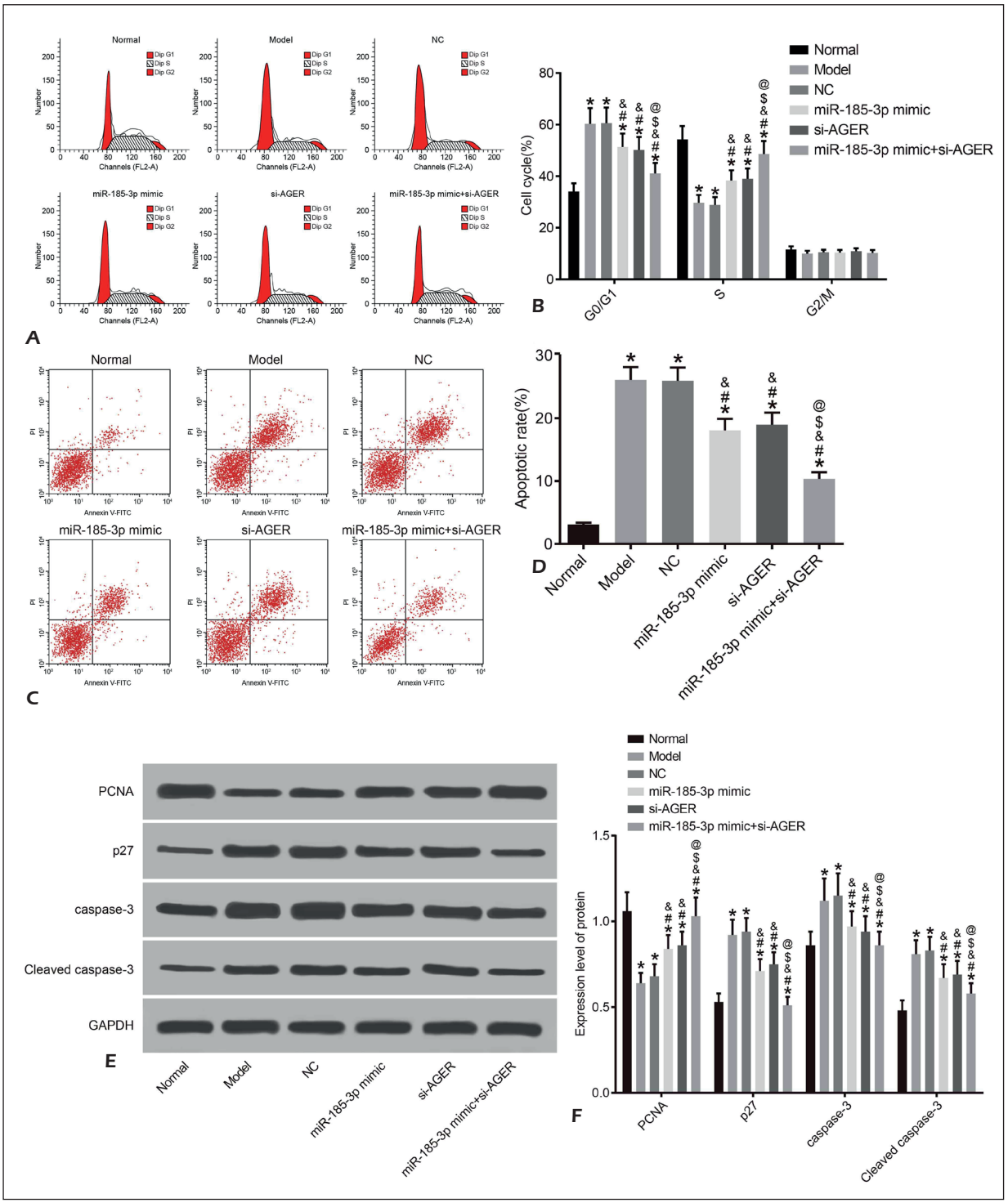

Figure 4. Detection of renal cell cycle and apoptosis and expression of protein in kidney tissues. **A**, Flow cytometry of cell cycle. **B**, Statistical results of renal cell cycle distribution in each group. **C**, Flow cytometry of cell apoptosis. **D**, Statistical results of apoptotic ratio of kidney cells in each group. **E**, Expression of protein by Western blotting. **F**, Protein expression in the kidney tissues of rats in each group. Compared with Normal group, $^{*}p<0.05$. Compared with Model group, $^{\#}p<0.05$. Compared with NC group, $^{\&}p<0.05$. Compared with miR-185-3p mimic group, $^{\$}p<0.05$. Compared with si-AGER group, $^{@}p<0.05$. AGER: advanced glycosylation end product receptor.

tent, Scr, and BUN content, were significantly improved. In addition, the content of MDA decreased, whilst CAT and SOD levels increased, which promoted the proliferation of kidney cells and inhibited apoptotic induction.

AGER strongly influences DN. Through the analysis of the TargetScanHuman, it was predicted that the binding sites between miR-185-3p and AGER were present, which was verified through Dual-Luciferase reporter assays[28-30]. qRT-PCR and Western blot analysis showed that, in comparison to the normal group, AGER mRNA and protein expression significantly increased in the kidneys of other groups. Compared to the model group, AGER gene and protein expression significantly decreased in the si-AGER and miR-185-3p mimic + si-AGER groups, whilst renal function indicators, including water intake, food intake, urinary protein, Scr, and BUN contents in the DN mice significantly improved in the si-AGER and miR-185-3p mimic + si-AGER groups. Meanwhile, MDA content decreased, and the levels of CAT and SOD increased, which promoted kidney cell proliferation and inhibited apoptosis. The combined treatment of miR-185-3p overexpression and AGER silencing produced additive effects over each monotherapy. We thus identified a negative regulatory relationship between miR-185-3p and AGER and indicated that the overexpression of miR-185-3p improves renal function in DN mice.

Conclusions

In this study, we demonstrated that miR-185-3p could improve the renal function of diabetic nephropathy mice by targeting AGER gene. This study further elucidated the development mechanism of diabetic nephropathy and laid a theoretical foundation for the treatment of clinical diabetic nephropathy. In order to further confirm the above results, we need to further supplement the clinical data. MicroRNAs modulate gene expression[31-35]. To date, it is unclear how miR-185-3p inhibits the post-transcriptional translation of AGER. The combined treatment of miR-185-3p mimics and si-AGER produced more beneficial effects that each respective monotherapy. This may be explained by other unidentified targets of miR-185-3p[36,37]. Moreover, whether miR-185-3p can be used in the clinic for the treatment of DN now requires further verification.

Conflict of Interests

The authors declare that they have no conflict of interests.

References

1) Wada J, Makino H. Innate immunity in diabetes and diabetic nephropathy. Nat Rev Nephrol 2016; 12: 13-26.
2) Miranda-Díaz AG, Pazarín-Villaseñor L, Andrade-Sierra J. Oxidative stress in diabetic nephropathy with early chronic kidney disease. J Diabetes Res 2016; 2016: 7047238.
3) Delić D, Eisele C, Schmid R, Baum P, Wiech F, Gerl M, Zimdahl H, Pullen SS, Urquhart R. Urinary exosomal miRNA signature in Type II diabetic nephropathy patients. PLoS One 2016; 11: e0150154.
4) Li J, Cai W, Zhang W, Zhu WF, Liu Y, Yue LX, Zhu LY, Xiao JR, Liu JY, Xu JX. Polymorphism 2184A/G in the AGER gene is not associated with diabetic retinopathy in Han Chinese patients with type 2 diabetes. J Int Med Res 2016; 44: 520-528.
5) Harbord NB, Winchester JF, Charen E, Ornillo C, Sheth N, Feinfeld D, Dubrow A. Diabetic Nephropathy. In: Poretsky L. (eds) Principles of Diabetes Mellitus. Springer International Publishing, 2017.
6) Jha JC, Thallas-Bonke V, Banal C, Gray SP, Chow BS, Ramm G, Quaggin SE, Cooper ME, Schmidt HH, Jandeleit-Dahm KA. Podocyte-specific Nox4 deletion affords renoprotection in a mouse model of diabetic nephropathy. Diabetologia 2016; 59: 379-389.
7) Barber AJ, Baccouche B. Neurodegeneration in diabetic retinopathy. Vision Res 2017; 139: 82-92.
8) Das A. Diabetic retinopathy: battling the global epidemic. Indian J Ophthalmol 2016; 57: 6669-6682.
9) Liu C, Li G, Ren S, Su Z, Wang Y, Tian Y, Liu Y, Qiu Y. MiR-185-3p regulates the invasion and metastasis of nasopharyngeal carcinoma by targeting WNT2B in vitro. Oncol Lett 2017; 13: 2631-2636.
10) Li J, Liu H, Zou L, Ke J, Zhang Y, Zhu Y, Yang Y, Gong Y, Tian J, Zou D, Peng X, Gong J, Zhong R, Huang K, Chang J, Miao X. A functional variant in GREM1 confers risk for colorectal cancer by disrupting a hsa-miR-185-3p binding site. Oncotarget 2017; 8: 61318-61326.
11) Kristensen H, Thomsen AR, Haldrup C, Dyrskjøt L, Høyer S, Borre M, Mouritzen P, Ørntoft TF, Sørensen KD1. Novel diagnostic and prognostic classifiers for prostate cancer identified by genome-wide microRNA profiling. Oncotarget 2016; 7: 30760-30771.
12) Rawal S, Munasinghe PE, Shindikar A, Paulin J, Cameron V, Manning P, Williams MJ, Jones GT, Bunton R, Galvin I, Katare R. Down-regulation of proangiogenic microRNA-126 and microRNA-132 are early modulators of diabetic cardiac microangiopathy. Cardiovasc Res 2017; 113: 90-101.
13) Tsitoura E, Wells AU, Karagiannis K, Lasithiotaki I, Vasarmidi E, Bibaki E, Koutoulaki C, Sato H, Spandidos DA, Siafakas NM, Sourvinos G, Antoniou KM. MiR-185/AKT and miR-29a/Collagen 1a pathways are activated in IPF BAL cells. Oncotarget 2016; 7: 74569-74581.

14) Ma D, Cao Y, Wang Z, He J, Chen H, Xiong H, Ren L, Shen C, Zhang X, Yan Y, Yan T, Guo F, Xuan B, Cui Z, Ye G, Fang JY, Chen H, Hong J. CCAT1 lncRNA promotes inflammatory bowel disease malignancy by destroying intestinal barrier via downregulating miR-185-3p. Inflamm Bowel Dis 2019; 25: 862-874.
15) Gits CM, van Kuijk PF, de Rijck JC, Muskens N, Jonkers MB, van IJcken WF, Mathijssen RH, Verweij J, Sleijfer S, Wiemer EA. MicroRNA response to hypoxic stress in soft tissue sarcoma cells: microRNA mediated regulation of HIF3α. BMC Cancer 2014; 14: 1-13.
16) Yin C, Yin C, Zhang G, Sun R, Pan X, Wang X, Li H, Sun Y. MiR-185-5p inhibits F-actin polymerization and reverses epithelial mesenchymal transition of human breast cancer cells by modulating RAGE. Mol Med Rep 2018; 18: 2621-2630.
17) Li L, Gao F, Zheng H, Jiang Y, Tong W, Zhou Y, Tong G. Utilizing host endogenous microRNAs to negatively regulate the replication of porcine reproductive and respiratory syndrome virus in MARC-145 cells. PLoS One 2018; 13: e0200029.
18) Singh J, Boopathi E, Addya S, Phillips B, Rigoutsos I, Penn RB, Rattan. Aging-associated changes in microRNA expression profile of internal anal sphincter smooth muscle: Role of microRNA-133a. Am J Physiol Gastrointest Liver Physiol 2016; 311: G964-G973.
19) Seo E, Kang H, Oh YS, Jun HS. Psoralea corylifolia L. seed extract attenuates diabetic nephropathy by inhibiting renal fibrosis and apoptosis in streptozotocin-induced diabetic mice. Nutrients 2017; 9: pii: E828.
20) Cooke JN, Bostrom MA, Hicks PJ. Polymorphisms in MYH9 are associated with diabetic nephropathy in European Americans. Nephrol Dial Transplant 2016; 27: 1505-1511.
21) Tagawa A, Yasuda M, Kume S. Impaired podocyte autophagy exacerbates proteinuria in diabetic nephropathy. Diabetes 2016; 65: 755-767.
22) Yu M, Liu Y, Zhang B. Inhibiting microRNA-144 abates oxidative stress and reduces apoptosis in hearts of streptozotocin-induced diabetic mice. Cardiovasc Pathol 2015; 24: S1054880715000770.
23) Lindhardt M, Persson F, Currie G, Pontillo C, Beige J, Delles C, von der Leyen H, Mischak H, Navis G, Noutsou M, Ortiz A, Ruggenenti PL, Rychlik I, Spasovski G, Rossing P. Proteomic prediction and Renin angiotensin aldosterone system inhibition prevention of early diabetic nephropathy in Type 2 diabetic patients with normoalbuminuria (PRIORITY): essential study design and rationale of a randomised clinical multicentre trial. BMJ Open 2016; 6: e010310.
24) Delic D, Eisele C, Schmid R, Luippold G, Mayoux E, Grempler R. Characterization of micro-RNA changes during the progression of type 2 diabetes in Zucker diabetic fatty rats. Int J Mol Sci 2016; 17: 665.
25) Zhu SM, Chen CM, Jiang ZY, Yuan B, Ji M, Wu FH, Jin J. MicroRNA-185 inhibits cell proliferation and epithelial-mesenchymal transition in hepatocellular carcinoma by targeting Six2. Eur Rev Med Pharmacol Sci 2016; 20: 1712-1719.
26) Huang Z, Zhu D, Wu L, He M, Zhou X, Zhang L, Zhang H, Wang W, Zhu J, Cheng W, Chen Y, Fan Y, Qi L, Yin Y, Zhu W, Shu Y, Liu P. Six serum-based miRNAs as potential diagnostic biomarkers for gastric cancer. Cancer Epidemiol Biomarkers Prev 2017; 26: 188-196.
27) Béres NJ, Kiss Z, Sztupinszki Z, Lendvai G, Arató A, Sziksz E, Vannay Á, Szabó AJ, Müller KE, Cseh Á, Boros K, Veres G. Altered mucosal expression of microRNAs in pediatric patients with inflammatory bowel disease. Dig Liver Dis 2017; 49: 378-387.
28) Gardner T, Chew E. Future opportunities in diabetic retinopathy research. Curr Opin Endocrinol Diabetes Obes 2016; 23: 91-96.
29) Labhade JD, Chouthmol LK, Deshmukh S. Diabetic retinopathy detection using soft computing techniques. 2016 International Conference on Automatic Control and Dynamic Optimization Techniques (ICACDOT), June, 2016, pp. 175-178.
30) Takasaki K, Babazono T, Ishizawa K. Relationship between diabetic nephropathy and depression: a cross-sectional analysis using the diabetes study from the Center of Tokyo Women's Medical University (DIACET). BMJ Open Diabetes Res Care 2016; 4: e000310.
31) Qin Y, Peng Y, Zhao W, Pan J, Ksiezak-Reding H, Cardozo C, Wu Y, Divieti Pajevic P, Bonewald LF, Bauman WA, Qin W. Myostatin inhibits osteoblastic differentiation by suppressing osteocyte-derived exosomal micro RNA-218: a novel mechanism in muscle-bone communication. J Biol Chem 2017; 292: 11021-11033.
32) Guo R, Nair S. Role of microRNA in diabetic cardiomyopathy: from mechanism to intervention Biochim Biophys Acta Mol Basis Dis 2017; 1863: 2070-2077.
33) Wei R, Yang Q, Han B, Li Y, Yao K, Yang X, Chen Z, Yang S, Zhou J, Li M, Yu H, Yu M, Cui Q. MicroRNA-375 inhibits colorectal cancer cells proliferation by downregulating JAK2/STAT3 and MAP3K8/ERK signaling pathways. Oncotarget 2017; 8: 16633-16641.
34) Krauskopf J, de Kok TM, Schomaker SJ, Gosink M, Burt DA, Chandler P, Warner RL, Johnson KJ, Caiment F, Kleinjans JC, Aubrecht J. Serum microRNA signatures as "liquid biopsies" for interrogating hepatotoxic mechanisms and liver pathogenesis in human. PLoS One 2017; 12: e0177928.
35) Flamand MN, Gan HH, Mayya VK, Gunsalus KC, Duchaine TF. A non-canonical site reveals the cooperative mechanisms of microRNA-mediated silencing. Nucleic Acids Res 2017; 45: 7212-7225.
36) Warnefors M, Mössinger K, Halbert J, Studer T, VandeBerg JL, Lindgren I, Fallahshahroudi A, Jensen P, Kaessmann H. Sex-biased microRNA expression in mammals and birds reveals underlying regulatory mechanisms and a role in dosage compensation. Genome Res 2017; 27: 1961-1973.
37) Naqvi S, Bellott DW, Lin KS, Page DC. Conserved microRNA targeting reveals preexisting gene dosage sensitivities that shaped amniote sex chromosome evolution. Genome Res 2018; 28: 474-483.